Co-refolding of a functional complex of Dengue NS3 protease and NS2B co-factor domain and backbone resonance...

Article *in* Protein Expression and Purification · July 2017

DOI: 10.1016/j.pep.2017.07.002

CITATIONS
0

READS
9

5 authors, including:

Tatiana Agback
Medivir

86 PUBLICATIONS **802** CITATIONS

SEE PROFILE

Protein Expression and Purification 140 (2017) 16–27

Contents lists available at ScienceDirect

Protein Expression and Purification

journal homepage: www.elsevier.com/locate/yprep

Co-refolding of a functional complex of Dengue NS3 protease and NS2B co-factor domain and backbone resonance assignment by solution NMR

Esmeralda Woestenenk [a, *], Peter Agback [b], Sofia Unnerståle [a], Ian Henderson [a], Tatiana Agback [a]

[a] Medivir AB, PO Box 1086, SE-141 22, Huddinge, Sweden
[b] Department of Molecular Sciences, Swedish University of Agricultural Sciences, PO Box 7015, SE-750 07, Uppsala, Sweden

ARTICLE INFO

Article history:
Received 25 April 2017
Received in revised form
30 June 2017
Accepted 6 July 2017
Available online 24 July 2017

Keywords:
Dengue virus
NS3 protease
Flavivirus protease
Refolding
Protein purification
Resonance assignment
Protein complex

ABSTRACT

A novel approach for separate expression of dengue virus NS3 protease and its NS2B cofactor domain is described in this paper. The two proteins are expressed in *E.coli* and purified separately and subsequently efficiently co-refolded to form a stable complex. This straightforward and robust method allows for separate isotope labeling of the two proteins, facilitating analysis by nuclear magnetic resonance (NMR) spectroscopy. Unlinked NS2B-NS3pro behaves better in NMR spectroscopy than linked NS2B-NS3pro, which has resulted in the backbone resonance assignment of the unlinked NS2B-NS3 complex bound to a peptidic boronic acid inhibitor.

1. Introduction

The incidence of dengue virus (DENV) has grown dramatically around the world in recent decades and constitutes a major threat to human health. With increased infection rates, aided by global warming, the growth of urban areas, and travel and trade, the virus is now endemic in more than 100 countries and not only restricted to tropical and subtropical regions. The World Health Organization (WHO) estimates that almost half of the world's population are at risk of acquiring DENV infection, with 50–100 million infections annually [1a]. Currently, prevention of dengue outbreaks mostly encompasses vector control [1a]. Dengvaxia®, a tetravalent dengue vaccine developed by Sanofi-Pasteur, has been approved in eleven countries for the prevention of dengue virus infection [1b]. However, there are risks associated with the vaccine in seronegative individuals, which might limit the use of the vaccine to use in high transmission risk settings [1]. No antiviral agents specifically targeting dengue virus are available today.

DENV belongs to the Flavivirus genus, a family that includes a number of human pathogens including yellow fever virus (YFV), West Nile virus (WNV), Zika virus (ZIKV) and tick-borne encephalitis virus (TBEV). DENV exists in four serotypes (DENV1, -2, -3, -4), all containing a single strand positive-sense RNA. The genome encodes three structural (C, prM, E) and seven non-structural (NS1, NS2A, NS2B, NS3, NS4A, NS4B, NS5) proteins that are translated as a single polypeptide chain. During viral replication the individual proteins are released by proteolytic processing by at least two different proteases, one of host and the other of viral origin [2]. The virally encoded serine protease (NS3pro) lies in the N-terminal domain of NS3, with NS2B serving as a cofactor in this dimeric protease. Full length NS2B is a membrane protein, but in vitro a hydrophilic segment of 40-residues is sufficient to form active NS2B-NS3pro [3]. The protease activity of the NS2B-NS3 dimer is essential for virus proliferation: NS3 mutant viruses with catalytically inactivating mutations in the protease active site are non-infectious [2]. The pivotal role of the NS2B-NS3 in DENV reproduction has made it an attractive target for antiviral interventions. The current work focuses on NS2B-NS3pro of the most prevalent

* Corresponding author.
E-mail address: esmeralda.woestenenk@medivir.com (E. Woestenenk).

http://dx.doi.org/10.1016/j.pep.2017.07.002
1046-5928/

dengue virus serotype, type 2 (DENV2).

A crystal structure of apo DENV2 NS2B-NS3pro was first determined by Erbel et al., in 2006 [4]. In this structure, NS2B is in the 'open state' and folds away from the active site (Fig. 1). A crystal structure of DENV3 NS2B-NS3pro in the presence of a substrate-like peptidic inhibitor, shows that the NS2B C-terminus associates with NS3pro such that it folds over to the active site and interacts directly with P2 and P3 of the peptidic inhibitor [5] (Fig. 1). This NS2B conformation is referred to as the 'closed' conformation. The C-terminal part of NS2B has been shown essential for proteolytic activity in both DENV [4,6–8] and WNV [9], therefore the closed conformation is thought to be the enzymatically active structure. Recent studies using NMR spectroscopy and paramagnetic labels suggest that NS2B predominantly adopts the closed conformation in solution, even in the absence of substrate-like inhibitors [10,11]. These findings suggest that the open state of ligand-free DENV NS2B-NS3pro observed in crystal structures may be the result of crystal packing.

As mentioned, a crystal structure of DENV3 protease in complex with a peptidic inhibitor has been reported [5], but DENV2 protease, sharing 67% sequence identity with DENV3 protease, has proven more difficult to crystallize in complex with inhibitors. NMR structures (2M9P, 2M9Q) of DENV2 protease in complex with a peptidic inhibitor were reported in the Protein Data Bank in 2014. A feature shared between these structures is the presence of a flexible, non-cleavable 9-residue linker (G_4-S-G_4) connecting a C-terminal segment of NS2B to NS3pro [13,14]. The presence of the linker provides a different set of constraints that may influence structure and activity compared to a more natural unlinked state. Knowledge about the structure and dynamics of a *trans*-acting form of a flaviviral NS2B-NS3pro is important for further rational drug design efforts.

A number of recent papers describe expression and purification of unlinked NS2B-NS3pro by different co-expression methods [10,15]. To our knowledge, two papers have reported refolding of DENV NS2B-NS3pro to this date. Yusof et al. describe a procedure for refolding of naturally linked NS2B-NS3pro [8], while a recent paper by Gupta et al. describes co-refolding of unlinked NS2B and NS3pro with a procedure that was not described in detail [16]. In the current paper, we describe an alternative and highly efficient approach for production of an unlinked NS2B-NS3pro protease from DENV2 by separate expression and subsequent co-refolding of the two domains; a strategy that had the advantage of differential isotope labelling which resulted in the backbone assignment of a peptidic inhibitor bound complex by solution NMR.

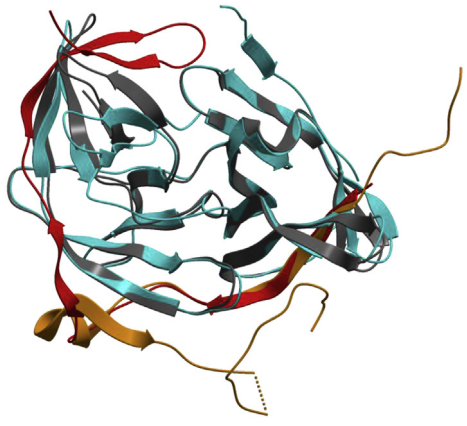

Fig. 1. Structural alignment of two crystal structures of linked NS2B-NS3pro illustrating the open and closed conformations of NS2B. The structure of the open conformation, 2FOM [4], shows DENV2 NS3pro in grey and NS2B in orange. The structure of the closed conformation, 3U1I [5], shows DENV3 NS3pro in cyan and NS2B in red. (For interpretation of the references to colour in this figure legend, the reader is referred to the web version of this article.)

2. Material and methods

2.1. Cloning of expression constructs

The sequence of DENV2 (strain TSV01) His-thrombin-NS2B-G_4SG_4-NS3pro based on the 2FOM structure [4] was ordered from Eurofins Genomics as a DNA sequence codon-optimized for *Escherichia coli* flanked by *Nde*I - *Xho*I sites for subcloning into pET21b (Novagen). The NS2B construct (containing amino acids 1394–1440 of the Dengue 2 polyprotein) was generated from the His-thrombin-NS2B-G_4SG_4-NS3pro construct by PCR; a stop codon was introduced at the C-terminus and it was subcloned into pET21b using *Nde*I – *Bam*HI sites. The full-length NS3pro (1–185; amino acids 1476–1660 of the polyprotein) construct was generated from the His-NS2B-G_4SG_4-NS3pro construct by PCR; a His_6 tag was introduced at the N-terminus (sequence MSHHHHHHS-NS3pro1-185) and it was subcloned into pET21b using *Nde*I – *Xho*I sites. To generate the truncated NS3pro(16–170) construct for crystallization, the full-length NS3pro sequence was shortened by 15 amino acids on each end by PCR, while introducing a His tag – TEV protease cleavage site sequence at the N-terminus. The new construct was generated by PCR in two steps. The first step was done with forward primer 5′GAGAACCTGTACTTCCAGGGTTCGGCAGAACTGGAAGATGGTGC3′ and reverse primer 5′CAGCGGCTCGAGTTATTTCTCGGTTTGGGCAATCGC3'. The product was then amplified again with the same reverse primer and forward primer 5′CCGCTCATATGTCTTCACATCATCATCACCATCATGAGAACCTGTACTTCCAGGG3'. The product was subcloned to pET21b using *Nde*I and *Xho*I sites.

NS2B with an N-terminal Gb1 tag [17] was ordered as a synthetic gene with codon optimization for *Escherichia coli* from Eurofins Genomics (Germany). The ordered sequence was MGSHHHHHH-SQYKLILNGKETTTEAVDAATAEKVFQYANDNGVDG-EWTYDDATKTFTVTE-KRR-ADLELERAADVRWEEQAEISGSS-PILSITISEDGSMSIKNEEEEQTL (dashes separate the different parts of the fusion protein: His tag, Gb1, NS3pro cleavage site, NS2B). The gene was subcloned to pET21b using *Nde*I and *Xho*I. No evidence of cleavage at the KRR site by NS3pro could be observed.

2.2. Protein expression and IMAC purification

Reagents were from Sigma (St. Louis, MO, USA) unless otherwise stated. Linked NS2B-NS3 was prepared as described in Erbel et al. [4]. NS2B and NS3pro were expressed separately in *Escherichia coli* expression strain BL21Star (DE3) (Life Technologies) at 37 °C and with 50 μg/ml carbenicillin as the selective antibiotic, either in Terrific Broth medium (MP Biomedicals) for unlabelled protein or in different isotopic labelling combinations in $^{1/2}H$, ^{15}N, $^{12/13}C$-labelled M9 medium [18] for labelled protein. Chemicals for isotope labelling (ammonium chloride, ^{15}N (99%), D-glucose, ^{13}C (99%), deuterium oxide) were purchased from Cambridge Isotope Laboratories, Inc. Protein expression was induced by adding isopropyl-b-D-thiogalactoside (IPTG) at a final concentration of 0.5 mM when OD_{600} was 1.5–2.5. The cultures were then incubated for another 3–4 h at 37 °C and the cells were harvested by centrifugation at 6000*g*. Purification of NS2B: lysis buffer containing 50 mM Tris pH 8.5 (4 °C), 20 mM imidazole and 5% glycerol was added to the cell pellet. Cells were resuspended and lysed using high pressure (1.7 kbar) using a Cell Disruptor (Constant Systems), followed by

centrifugation at 28,000×*g* to remove cell debris. NS2B was purified from the supernatant by batch binding to Ni^{2+} Sepharose 6 Fast Flow (GE Healthcare) for 1 h at 4 °C. The protein was eluted with an elution buffer of the same composition as the lysis buffer, only with 0.5 M imidazole added. Purification of NS3pro: NS3pro was expressed in the insoluble fraction of the cell as inclusion bodies. Cells were resuspended in PBS and lysed at high pressure. The lysate was centrifuged at 10,000×*g* and the supernatant was discarded. The pellet was washed three times with wash buffer: 50 mM Hepes pH 7.5, 1 M urea and 2% Triton X-100, by homogenizing the pellet in the buffer with a YellowLine DI25 basic (IKA) motorized homogenizer, followed by centrifugation at 10,000×*g*. The pellet was solubilized overnight on a rolling board in solubilizing buffer: 8 M urea, 50 mM Tris pH 7.6 (RT), 20 mM imidazole, 0.5 M NaCl. After solubilization, the solution was centrifuged at 50,000×*g*, and NS3pro was purified from the supernatant with Ni^{2+} Sepharose 6 Fast Flow. Protein was eluted with denaturing elution buffer: 50 mM Tris pH 8.0 (RT), 8 M urea, 0.5 M imidazole. Typical yields after IMAC were 10–20 mg NS2B per liter culture medium, and 50–80 mg NS3pro per liter culture medium.

2.3. Co-refolding of NS2B and NS3 and purification

NS2B and NS3pro were co-refolded by one-step dialysis overnight at 4 °C in a 2:1 M NS2B:NS3pro ratio to maximize formation of the active complex. The refolding buffer was 25 mM Tris pH 8.5 (pH set at 4 °C), 5% glycerol, 100 mM NaCl. Thrombin (GE Healthcare) and/or TEV protease (produced in house according to [19]) was added to a dialysis cassette (3500 or 7000 MWCO Slide-A-Lyzer, Thermo Fisher Scientific) to cleave off the His tag from NS2B and/or NS3pro. Thrombin could be added directly, and did not lose activity in the high concentration urea solution of the dialysis cassette, while TEV protease was added 1 h after starting the dialysis. After refolding the solution was centrifuged at 50,000×*g* to remove any precipitate or particles. Refolding yield was determined by measuring protein concentration of the two IMAC pools (NS2B: ε 5,500, MW 7.7 kDa; NS3pro: ε 36,400, MW 21.0 kDa) before refolding and comparing that to the protein concentration after refolding and centrifugation (complex: ε 41,940, MW 28.7 kDa), using a Nanodrop 1000 instrument (Thermo Scientific). The complex was then purified on an ÄKTA Explorer (GE Healthcare) by size exclusion on a HiLoad Superdex 200 column (GE Healthcare) in SEC buffer: 50 mM Tris pH 8.5 (4 °C), 5% glycerol, 50 mM NaCl. Typical refolding yields were 70–80%. Molar ratio was extremely important for refolding yield. Anything less than a 2:1 ratio of NS2B:NS3pro increased the formation of precipitate and lowered the refolding yield. Apart from the molar ratio, another factor important for the yield of correctly folded complex was the freshness of IMAC-purified NS3pro. NS3pro was purified by IMAC under denaturing conditions and since yields were so high, the material that was not immediately used for refolding was stored at 4 °C. The storage did not affect the refolding yield initially (i.e. the first 2–3 weeks), but over time more NS3pro became aggregated and was thus prevented from refolding into a functional complex with NS2B. IMAC-purified NS2B was stored at −20 °C indefinitely without affecting refolding yield.

2.4. Biochemical assay

Activity assays were carried out on a 96-well plate (white Cliniplate, Thermo Fisher Scientific Oy, Vantaa, Finland) in 50 mM HEPES, pH7.4, 150 mM NaCl, 10% ethylene glycol, 0.05% BSA, 0.0016% Brij-58 with 80 nM enzyme using 20 μM Bz-nle-Lys-Arg-Arg-AMC (Bachem, Bubendorf, Switzerland) as substrate. Reagents were from Sigma (St. Louis, MO, USA) unless otherwise stated.

5 μl of 200 μM substrate in buffer and 2.5 μl of compound in DMSO or DMSO control were added to the plate. 42.5 μl of 94 μM enzyme in buffer was added to start the reaction. Fluorescence was read every 30 s for 30 min at 390 nm excitation and 460 nm emission in a Fluorskan Ascent plate reader (Thermo Fisher Scientific Oy, Vantaa, Finland). Rates were fitted in the Ascent software and exported as Excel files. The rates were imported into GraphPad Prism (GraphPad Software Inc, La Jolla, CA, USA) and fitted to the standard three parameter IC_{50} equation.

2.5. Protease inhibitors

The NS3pro inhibitors Bz-Nle-Lys-Arg-Arg-B$(OH)_2$ and 2,6-di-fluoro-Bz-Nle-Lys-Arg-Arg-CF3-ketone used in this study were synthesized according to the reaction schemes published in the original paper [20].

2.6. Preparation of NMR samples

The NS2B-NS3pro complex was concentrated in disposable centrifugal concentrators (e.g. Amicon Ultra centifugal filter units) with a molecular weight cut-off of 10 kDa. The complex was stable during concentration and no leakage of NS2B occurred. Buffer was exchanged using gravity flow desalting columns (GE Healthcare). The NMR buffer contained 20 mM deuterated MES (Cambridge Isotope Laboratories, Inc), 100 mM NaCl, 5 mM $CaCl_2$, 0.02% NaN_3, pH 6.5. The buffer-exchanged protein was concentrated to at least 0.3 mM. The ternary NS2B-NS3pro-inhibitor complex was prepared in two steps. Firstly, the inhibitor 2,6-di-fluoro-Bz-Nle-Lys-Arg-Arg-CF_3-ketone was titrated to a final concentration of 1 mM by adding 3 μL to the NS2B-NS3pro sample from a 100 mM stock solution in D_2O. The formation of bound complex was monitored by the reduction of the ^{19}F signal of unbound inhibitor and appearance of the broad signal corresponding to bound inhibitor. Secondly, the Bz-Nle-Lys-Arg-Arg-B$(OH)_2$ inhibitor was added to the sample to replace the Bz-Nle-Lys-Arg-Arg-CF_3-ketone inhibitor, which was monitored over time until the ^{19}F signal representing the bound inhibitor had disappeared and the ^{19}F signal of unbound inhibitor had fully reappeared.

2.7. NMR spectroscopy

NMR experiments were acquired on Bruker Avance III spectrometers operating at 14.1 and 16.4 T at a temperature of 298 K. Backbone assignment was performed as described previously [21]. Briefly, for backbone assignment, transverse relaxation optimized spectroscopy (TROSY) [22–24] versions of HNCO [25], HNCA [25], HN(CO)CA [26], HNCACB [26] and HN(CO)CACB [26], using gradient echo-anti echo TROSY and ^2H-decoupling, were acquired together with a 2D ^1H-^{15}N TROSY. The backbone assignment was performed manually in CcpNmr Analysis 2.2.2 [27]. In order to estimate the secondary structure of the NS2B-NS3pro complex with the Bz-Nle-Lys-Arg-Arg-B$(OH)_2$ inhibitor, random coil chemical shifts [28] were subtracted from the $^{13}C'$, $^{13}C\alpha$ and $^{13}C\beta$ chemical shifts. Chemical shift perturbation (CSP) was defined as the distance between two cross peaks in Hz, obtained as the square root of the sum of quadratic using DANGLE [38]. ^1H and ^{15}N chemical shift deviations in Hz.

To investigate backbone dynamics, longitudinal (T_1) and transverse (T_2) relaxation times and steady state heteronuclear NOEs ^{15}N CPMG-based relaxation dispersion experiments were measured for each ^1H-^{15}N vector in ^{15}N,^{13}C, ^2H -labelled NS2B-NS3pro in complex with Bz-Nle-Lys-Arg-Arg-B$(OH)_2$. T_1, T_2 and NOEs were determined using sensitivity enhanced TROSY versions of standard pulse

sequences [29]. T_1 relaxation was determined from the following series of relaxation delays: 10, 90, 192, 320, 480, 690, 980, 1220 and 1444 ms. T_2 relaxation was measured using CPMG delays of 8, 16, 24, 32, 40, 48, 56, 64, 72 and 88 ms. One of each of the T_1 and T_2 experiments was repeated in order to estimate the error in values and fitting, which was set to 2%. The same error was used for the NOE experiment. ^{15}N CPMG-based relaxation dispersion experiments were performed as described in the publication [30]. All spectra were evaluated using Topspin 3.2 and Dynamics Center 2.1 (Bruker), where T_1 and T_2 data are fitted to an exponential decay, while NOEs are calculated by dividing the intensity of the ^1H-^{15}N peaks in a NOE-enhanced spectrum by the corresponding intensities in an unsaturated spectrum. The relaxation parameters at two fields (only one field for NS3pro) were fitted using the Lipari-Szabo model-free approach with a NH bond length of 1.04 Å and a CSA of −160 ppm to obtain order parameters, S^2, and the fast internal correlation time, τE. Chemical shift index (CSI) was calculated according to the original method described in Wishart et al. [31].

2.8. Accession numbers

The NMR chemical shifts and assignment have been deposited to the BioMagResBank with accession code **26996**.

3. Results and discussion

3.1. Expression and purification

In this study a co-refolding approach is presented that produces unlinked NS2B-NS3pro protease from DENV2. Initially, we focused on a covalently linked NS2B-NS3pro with 9 residue G_4SG_4 linker [13,14](Fig. 2a and Supplementary Fig. 1). An apo structure of active protease was obtained that was very similar to other available structures. However, a screen of a small molecule compound library generated an abnormally high amount of hits, which prompted us to question the biological relevance of the covalent construct. In addition, no structure of inhibitor-bound NS2B-NS3pro could be obtained despite numerous attempts to crystallize the complex. We also observed by NMR spectroscopy and SDS-PAGE that over time, the protein was not stable in solution, indicating auto-proteolysis (Fig. 2b). The proteolytic fragments were not further analysed, but we speculated that the covalent linker, originally designed to give a more stable protease complex [13], did not actually result in a fusion protein that 1) was stable enough and behaved well enough for NMR spectroscopy, and 2) could not be crystallized together with a substrate-like inhibitor.

This prompted the design of an unlinked NS2B-NS3pro complex. Constructs for unlinked NS2B and NS3pro were generated from the His-thrombin-NS2B-G_4SG_4-NS3pro construct by PCR (Fig. 2a and Supplementary Fig. 1). The two proteins were expressed separately at 37 °C; NS2B in the soluble fraction and NS3pro as inclusion bodies. Expression of NS2B lowered the growth rate of the host cells but yielded around 10 mg per liter culture after IMAC purification, which was sufficient for enzymatic and structural studies. It was attempted to reduce the toxicity of NS2B expression by adding an N-terminal Gb1 tag [17] (see cloning paragraph for details) but no improvement of expression was observed, and the Gb1-NS2B construct was abandoned. NS3pro expressed to high levels in inclusion bodies and yielded 50–100 mg per liter culture after IMAC purification. Both proteins have an N-terminal His_6 tag and were purified by IMAC (Fig. 2c). It can be observed from Fig. 2c that NS2B migrates slower through the gel after removal of the His tag by thrombin digestion. Thrombin digestion lowers the pI of NS2B from 4.6 to 3.7, rendering it very acidic. This and its small size (5.9 kDa after tag removal) may influence its behavior in SDS-PAGE. The mass of NS2B was confirmed by mass spectrometry (data not shown).

Refolding was done by mixing NS2B and NS3pro in a 2:1 M ratio. Initial experiments were done at a 1:1 or 1.5:1 NS2B:NS3pro ratio, but increasing the ratio to 2:1 resulted in substantially lower levels of precipitation in the refolding reactions, and therefore consistently higher yields of active complex (Table 1). Generally, the yield in the refolding step was 70–80%. Refolding and simultaneous tag cleavage was performed by overnight dialysis of the protein mixture to a buffer without urea. Thrombin could be added directly to the input mixture and tolerated the brief exposure to high urea concentrations without losing any activity. TEV protease was less tolerant of high urea concentrations and was added to the refolding reaction later. An analysis was performed of variables, other than NS2B:NS3 ratio, which influenced refolding yield. Our hypothesis was that total protein concentration during refolding as well as input concentration of urea could be of importance for the refolding yield. High protein concentration was thought to result in more precipitation, but as can be seen in Fig. 3, similar yields were obtained with protein concentrations up to ca. 5 mg/ml, while in general refolding protocols tend to keep protein concentrations as low as possible to avoid misfolding and precipitation. For example, while we did observe light precipitation in the highest (5.2 mg/ml) concentration, as opposed to no precipitation in the lowest concentration (1.2 mg/ml), they resulted in 76% and 74% refolding yield, respectively (Fig. 3). This precipitation was light compared to the heavier precipitation observed in the initial 1:1 refolding experiment.

Similarly, our hypothesis was that a low initial urea concentration might cause NS3pro to precipitate before being able to form a stable complex with NS2B, but as depicted in Fig. 3, the lowest initial urea concentration (1.3 M) and the highest initial urea concentration (4.5 M) yielded very similar refolding yields: 79% and 84%, respectively. It would be interesting to investigate the process in more detail using a fractional factorial screen, but this was beyond the scope of the current study. We concluded that this co-refolding approach is simple, robust and tolerant of significant variation in parameters such as protein concentration and urea concentration as long as the 2:1 NS2B:NS3pro ratio is kept.

The complex was further purified by gel filtration and eluted as a single peak containing both domains (Fig. 4a). Analysis of the gel filtration fractions of NS2B-NS3pro shows a slightly shifted elution of NS2B towards the end of the peak; however, concentration of the protein after gel filtration using a concentrator with a 10 kDa cut-off never resulted in any leakage of NS2B. TruncNS3pro behaved like full-length NS3pro in purification, but was less stable in the complex over time. Linked NS2B-NS3pro could be crystallized using the protocol by d'Arcy et al. [32], and a structure of 1.6 Å was obtained (data not shown). Numerous attempts were made to soak and co-crystallize the protein with peptidic inhibitors but none were successful. Crystallization of NS2B-NS3pro by itself or in the presence of peptidic inhibitors was never successful in our hands, but diffracting crystals of NS2B-truncNS3pro were obtained and a 3.5 Å resolution structure in complex with the boronic acid peptidic inhibitor was obtained that showed the inhibitor covalently bound to the catalytic serine, while the overall conformation of the complex was structurally very similar to previously published closed conformations of linked DENV3 and WNV proteases (data not shown) [4,5].

3.2. Kinetic activity determination

The proteolytic activity of the co-refolded protease complex is very similar to the covalently linked NS2B-NS3pro protease

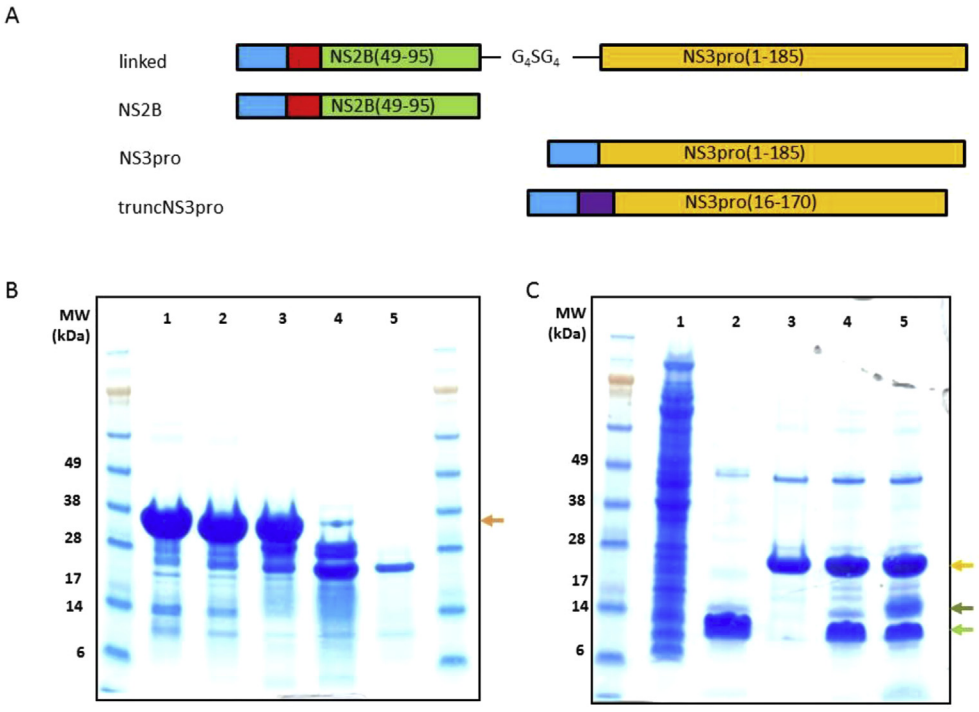

Fig. 2. Constructs and purification of DENV2 NS2B and NS3pro. A) Constructs of DENV2 NS2B and NS3pro. All constructs have an N-terminal His_6 tag (cyan). The linked construct is based on the 2FOM structure and has a thrombin cleavage site (red) after the His tag [4]. The NS2B construct is completely identical to the NS2B part of the linked construct. The NS3pro construct has a non-cleavable N-terminal His_6 tag and has been used in NMR studies and enzymatic assays. The truncated construct, truncNS3pro, was generated for X-ray crystallography and contains an N-terminal His_6 tag followed by a TEV protease cleavage site (purple). B) Instability of the linked NS2B-NS3pro construct over time shown by SDS-PAGE. The full-length protein is indicated with an orange arrow and migrates just below the 38 kDa marker band. Lanes: 1 – directly after size exclusion chromatography and concentration; 2 – after 24 h incubation at RT; 3 – after 48 h incubation at RT; 4 – after 96 h incubation at RT; 5 – after 1 week incubation at RT. C) Purification and refolding of unlinked NS2B-NS3pro shown by SDS-PAGE. NS3pro is indicated with a yellow arrow; NS2B is indicated with light and dark green arrows. Lanes: 1 – unbound protein after IMAC of NS2B; 2 – NS2B eluted from Ni Sepharose; 3 – NS3pro eluted from Ni Sepharose; 4 – NS2B-NS3pro co-refolded; 5 – NS2B-NS3pro co-refolded, N-terminal His_6 tag of NS2B partially cleaved off by thrombin, changing the migration of NS2B on SDS-PAGE. (For interpretation of the references to colour in this figure legend, the reader is referred to the web version of this article.)

Table 1
List of independent co-refolding experiments of NS2B and NS3pro with concentrations and yields. The asterisks (*) indicate experiments where no tag cleavage by thrombin was performed.

Molar ratio (NS2B: NS3pro)	Concentration NS2B (mM)	Concentration NS2B (mg/ml)	Input volume NS2B (ml)	Concentration NS3pro (mM)	Concentration NS3pro (mg/ml)	Input volume NS3pro (ml)	Reaction volume (ml)	Input urea concentration (M)	Protein concentration during refolding (mg/ml)	Yield after refolding (%)	Precipitate during refolding (y/n)
1: 1	0.080	0.62	6.0	0.078	1.64	4.0	10.0	3.2	2.26	66*	y
1.5: 1	0.076	0.59	8.0	0.048	1.01	8.0	16.0	4.0	1.60	84*	y
2: 1	0.063	0.49	8.0	0.032	0.67	7.1	15.1	3.8	1.15	74*	n
2: 1	0.193	1.49	8.0	0.090	1.88	4.0	12.0	2.7	3.36	62	n
2: 1	0.134	1.03	8.0	0.068	1.42	2.7	10.7	2.0	2.45	69	n
2: 1	0.129	1.00	6.0	0.062	1.30	1.8	7.8	1.8	2.29	79	n
2: 1	0.288	2.22	8.0	0.144	3.03	10.0	18.0	4.4	5.2	76	y
2: 1	0.165	1.27	10.0	0.077	1.63	2.9	12.9	1.8	2.9	78	y
2: 1	0.119	0.92	9.0	0.055	1.15	1.7	10.7	1.3	2.1	76	y
2: 1	0.227	1.59	4.5	0.113	2.42	5.8	10.3	4.5	4.0	75	y

analogue (Fig. 4b). Addition of excess NS2B to the reaction had no effect on the activity of unlinked NS2B-NS3 (data not shown). This indicates that the unlinked NS2B-NS3pro complex is indeed tightly associated in a 1:1 ratio even in absence of either substrate or inhibitor.

Bz-Nle-Lys-Arg-Arg-$B(OH)_2$ has an IC_{50} of 38 nM against linked NS2B-NS3 (Supplementary Fig. 2), which corresponds to the value measured by Yin et al. [20]. It was measured to have an EC_{50} of 44 μM on DENV2-infected Huh7 cells (data not shown). 2,6-di-fluoro-Bz-Nle-Lys-Arg-Arg-CF_3-ketone has an IC_{50} of 19 μM against linked NS2B-NS3pro (Supplementary Fig. 2). The inhibition of linked versus unlinked NS2B-NS3pro by the tetrapeptidic inhibitors in our compound library correlated very well; the two proteins behaved largely the same in the enzymatic assay (Supplementary Fig. 2). This was a surprising find to us as our initial hypothesis was that the linker would have a negative effect on protease activity; the effect of the nonnative linker on the enzymatic activity of the protease may thus be negligible.

3.3. Linked versus unlinked NS2B-NS3pro in NMR spectroscopy

We analysed and compared the ^{1}H-^{15}N TROSY spectra of linked

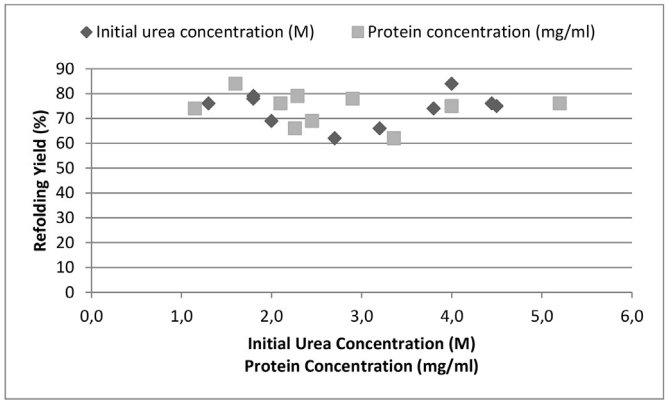

Fig. 3. Graphical representation of two variables in the refolding reaction. Total protein concentration (mg/ml) during refolding and initial urea concentration (M) are plotted against refolding yield (%). The x-axis has two units: initial urea concentration (M; dark grey diamonds) and protein concentration (mg/ml; light grey squares).

vs unlinked NS2B-NS3pro. The linker was found to have an unfavourable effect on the dynamics of the protein, resulting in broadening of cross peaks, especially (but not only) in the area around 9–10 ppm of the proton chemical shift (Fig. 5a). Comparatively, the spectrum for unlinked NS2B-NS3pro counts more well-resolved cross peaks and the cross peaks are to a higher extent of similar intensity (Fig. 5b). A similar improvement of spectral quality was observed by Kim et al. [10]. Fig. 5b also shows the advantage of differential labelling; especially the NS2B spectrum has basically no overlapping resonances. This showed convincingly that the unlinked complex was more amenable to structural studies by NMR spectroscopy. The spectral quality of the ^{1}H-^{15}N TROSY of unlinked NS2B-NS3pro is good enough for applications such as fragment screening and analysis of fragment binding by chemical shift perturbation. We observe similar locations of characteristic peaks in the ^{1}H-^{15}N TROSY of our co-refolded unlinked NS2B-NS3pro to previously published results for co-refolded and co-expressed unlinked NS2B-NS3pro [10,11,16].

3.4. NS2B-NS3pro backbone resonance assignment

The unlinked NS2B and NS3pro constructs allowed us to label the protease and the cofactor in different combinations to facilitate backbone resonance assignment by NMR spectroscopy. Three differently labelled non-covalent complexes were prepared: (1) ^{15}N,^{13}C,^{2}H-labelled NS2B with unlabelled NS3pro, (2) ^{15}N,^{13}C, ^{2}H-labelled NS3pro with unlabelled NS2B and (3) uniformly ^{15}N,^{13}C,^{2}H-labelled NS2B-NS3pro.

Without a potent inhibitor present, NS2B-NS3pro is not stable enough in the NMR sample conditions to perform the lengthy 3D experiments needed for assignment. This had also been observed for linked NS2B-NS3pro. Since our interest was mostly focused on protein – inhibitor interactions we did not investigate the stability of the sample any further. Our general observation was that the sample was stable for at least two days at 25 °C. Another hurdle for assignment is that some of the cross peaks in the ^{1}H-^{15}N TROSY spectrum are present as multiple peaks with varying intensities.

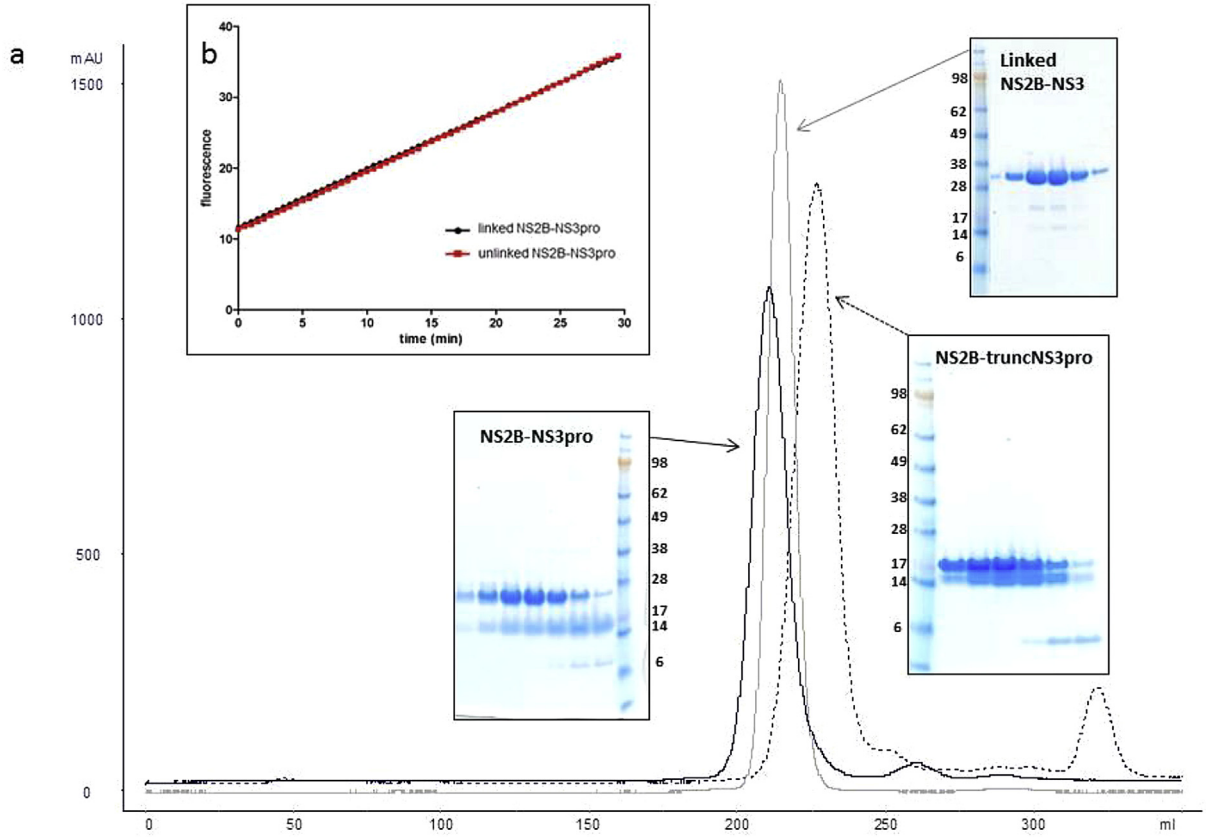

Fig. 4. Purification of NS2B-NS3pro and determination of proteolytic activity. A) Gel filtration profiles of various Dengue protease constructs and corresponding SDS gels of the fractions covering the A_{280} peaks. The X-axis shows elution volume in ml; the Y-axis shows A_{280} in mAU. The column that was used is a HiLoad 26/60 Superdex 200 pg (GE Healthcare). The solid dark profile is NS2B-NS3pro(1–185). The light grey profile represents linked NS2B-NS3pro; the dotted profile is NS2B/truncNS3pro. B) Comparison of enzymatic activity of linked (black dots) and unlinked (red squares) NS2B-NS3pro. The proteolytic activity was measured over time with substrate Bz-nle-Lys-Arg-Arg-AMC at pH 7.4. (For interpretation of the references to colour in this figure legend, the reader is referred to the web version of this article.)

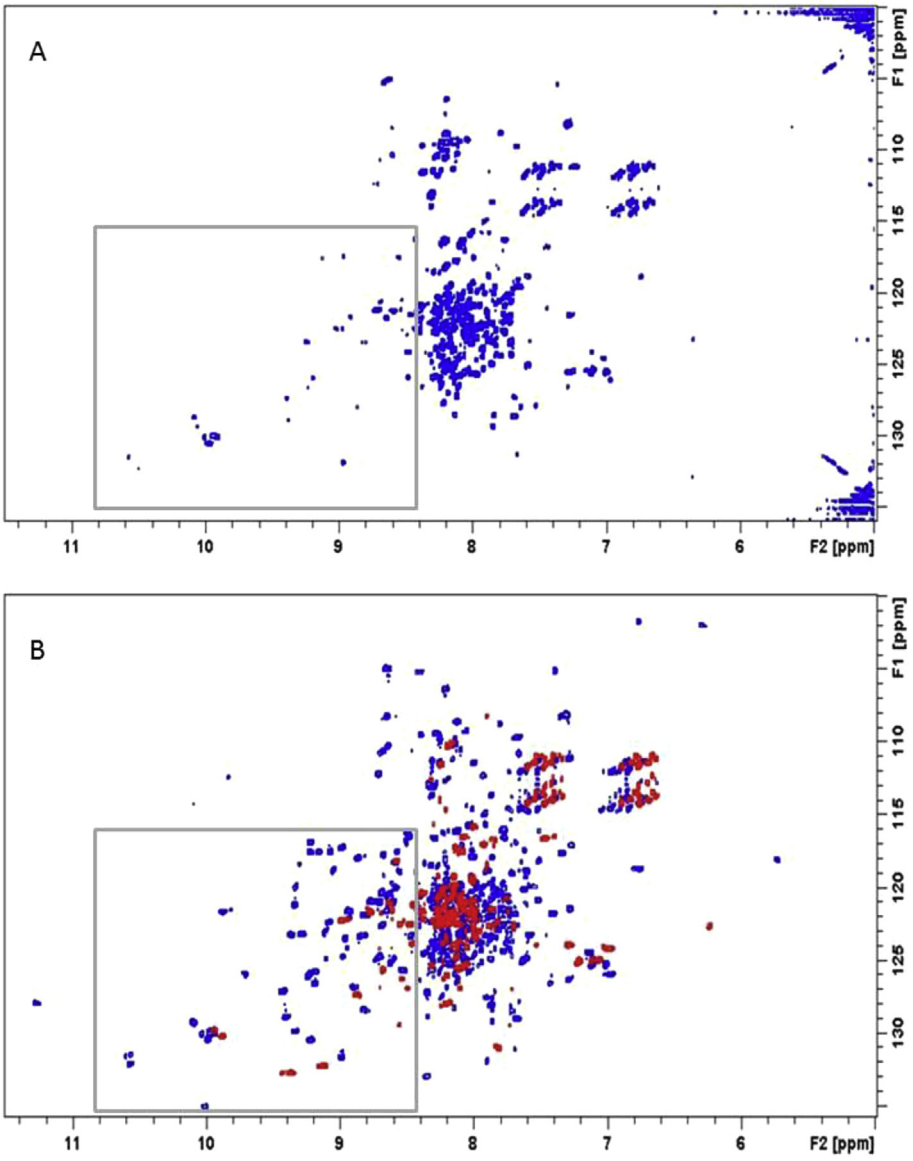

Fig. 5. ^{1}H-^{15}N TROSY spectra of linked (A) and unlinked (B) NS2B-NS3pro. No inhibitors were present in these experiments. A) Many cross peaks of linked NS2B-NS3pro, in particular in the boxed area, are broadening below detection due to the slow conformation exchange between multiple forms. B) In the same area, the cross peaks of unlinked NS2B-NS3pro are well resolved and could be assigned. This picture is a superposition of ^{15}N labelled NS2B (red; with unlabelled NS3) and ^{15}N labelled NS3(blue; with unlabelled NS2B). Noteworthy some resonances of amino moieties, e.g. Asn/Gln side-chain amides are not fully attenuated in TROSY spectrum and are presented as eight possible multiplets for each amide proton. The possible explanation could be found in Refs. [33,34]. See Fig. 6 for NS2B assignments and Supplementary Fig. 3 for NS3pro assignments, both in the presence of inhibitor. Free NS2B-NS3pro was not assigned. (For interpretation of the references to colour in this figure legend, the reader is referred to the web version of this article.)

Indeed, the number of cross peaks in the ^{1}H-^{15}N spectrum for NS2B (Fig. 6, blue spectrum) exceeds the number of expected cross peaks, indicating that in unlinked NS2B-NS3pro NS2B adopts a few stable conformations in different ratios. In linked NS2B-NS3pro these residues are not detectable due to signal broadening (Fig. 5A).

Several tetrapeptide inhibitor ligands were added to the protein complex in the hope that they would stabilize the conformation of the complex and lead to a spectrum more amenable to assignment. Two of these inhibitors are described in this study: a 2,6-di-fluoro-Bz-Nle-Lys-Arg-Arg-CF_3-ketone with 19 μM IC_{50} and a Bz-Nle-Lys-Arg-Arg-$B(OH)_2$ inhibitor with 38 nM IC_{50} on the enzyme complex. Addition of the weak inhibitor 2,6-di-fluoro-Bz-Nle-Lys-Arg-Arg-CF_3-ketone leads to minimal change in the ^{1}H-^{15}N correlation spectrum of NS2B (Fig. 6, red spectrum). A few cross peaks were still doublets even though inhibitor was confirmed to be bound to the protein through the detection of ^{19}F resonances of bound and unbound complexes (data not shown). The addition of the nM potency inhibitor Bz-Nle-Lys-Arg-Arg-$B(OH)_2$ significantly stabilized the complex, resulting in a spectral quality that was adequate for further NMR studies (Fig. 6, green spectrum). Residues Arg55, Arg60 and Glu62 are single peaks in the presence of the boronic acid inhibitor. The improved spectral quality upon binding of the boronic acid inhibitor allowed us to proceed with the assignment of the NMR resonances.

The protein backbone resonances in NS2B were sequentially assigned for residues Ala49- Gln93 (Fig. 6); HN (92%), N (92%), Cα (92%), and C' (90%). In addition, NS3pro was assigned; HN (85%), N (85%), Cα (94%) and C' (66%). The assigned ^{1}H-^{15}N TROSY spectrum for NS3pro is presented in Fig. S3 of the supplementary material. In Fig. S4 the secondary structure analysis for NS2B is presented. The

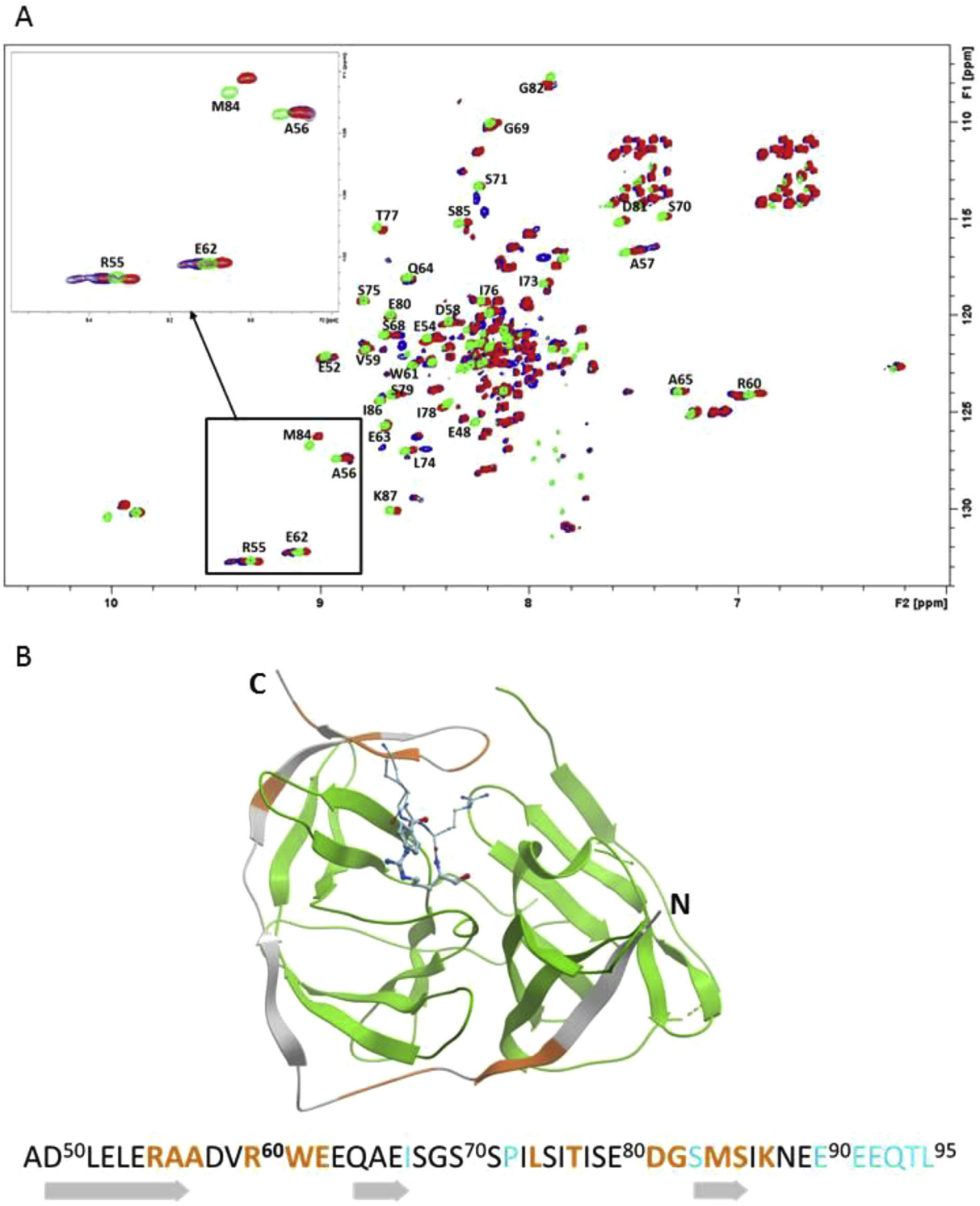

Fig. 6. Changes in NS2B conformation upon binding of a potent inhibitor. A) The $^{1}H^{15}N$ -TROSY of NS2B in the unlinked NS2B-NS3pro complex. NS2B is $^{15}N^{13}C^{2}H$ labelled and NS3pro is unlabelled. Colouring in spectrum: apo (blue), 2,6-di-fluoro-Bz-Nle-Lys-Arg-Arg-CF_3-ketone (red) and Bz-Nle-Lys-Arg-Arg-$B(OH)_2$ (green). Some of the cross peaks are shown in more detail in the expanded box. B) Residues with the largest chemical shift are mapped on the 3U1I structure [5]. NS3pro is shown in green, NS2B is shown in grey (the N- and C-termini are indicated in the figure with N and C, respectively), and residues that show the largest change in chemical shift upon inhibitor binding are marked in the structure and the sequence below in orange (cut off: 20 Hz or larger change). The inhibitor Bz-nKRR-H is shown to indicate the location of the active site. The image was made with ICM-Pro (Molsoft). The amino acid sequence of NS2B is displayed below the structure, with the secondary structure mapped to the sequence (see Supplementary Fig. S4 for secondary structure analysis). Unassigned residues are marked in the NS2B amino acid sequence in cyan. (For interpretation of the references to colour in this figure legend, the reader is referred to the web version of this article.)

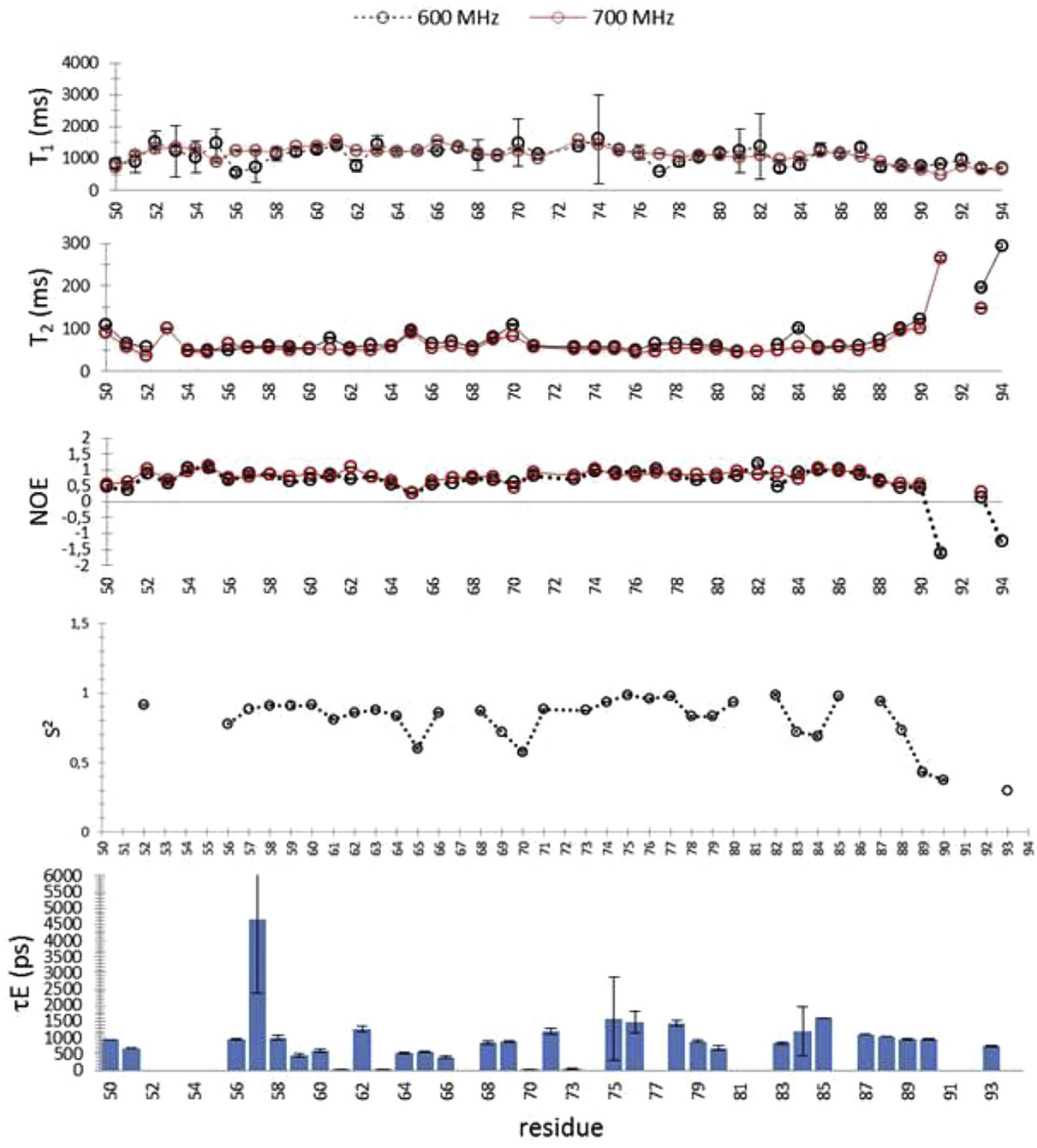

Fig. 7. Longitudinal (T_1) and transverse (T_2) relaxation times and steady state heteronuclear NOEs for ^{15}N,^{13}C,^{2}H-labelled NS2B with unlabelled NS3pro and Bz-Nle-Lys-Arg-Arg-$B(OH)_2$ at two different fields. General order parameter squared (S^2) is fitted to the data by the Modelfree approach. A S^2 value of 1 is indicative of a rigid ^{15}N-H vector, while a S^2 value of 0 is indicative of total flexibility. τE: correlation time of the fast internal motion of the ^{15}N of each residue.

secondary structure calculated from the chemical shift data corresponds well to our X-ray crystallography data (not published). For NS3pro, the secondary structure analysis is shown in Fig. S5.

3.5. NS2B conformational change upon interaction with a strong active site inhibitor

Chemical shift perturbation (CSP) of cofactor NS2B induced by ligand Bz-Nle-Lys-Arg-Arg-$B(OH)_2$ binding is shown in Fig. 6a. Cross peaks between ^{1}H and ^{15}N nuclei of the amide bonds showing significant CSP (>20 Hz) are mapped on a DENV3 structure and highlighted in the sequence of NS2B below the spectrum in orange (Fig. 6b). There are two major areas where chemical shifts of NS2B change upon binding the inhibitor: residues 55–62 and 74–87. For most NS2B resonances, these chemical shift perturbations are likely to be the result of the structural rearrangement of NS2B upon inhibitor binding. Gly82 and Met84, two of the residues with the largest shift, are the only two NS2B residues that have been observed in crystal structures to make direct contact with substrate-like inhibitors very similar to our boronic acid inhibitor [5,35]. Many of the chemical shift changes occur in the β-hairpin, where the loop between the two β-strands is around residues 79–81. While we have not investigated NS2B or NS3pro in the inhibitor-free state in depth, we observed that NS2B exists in

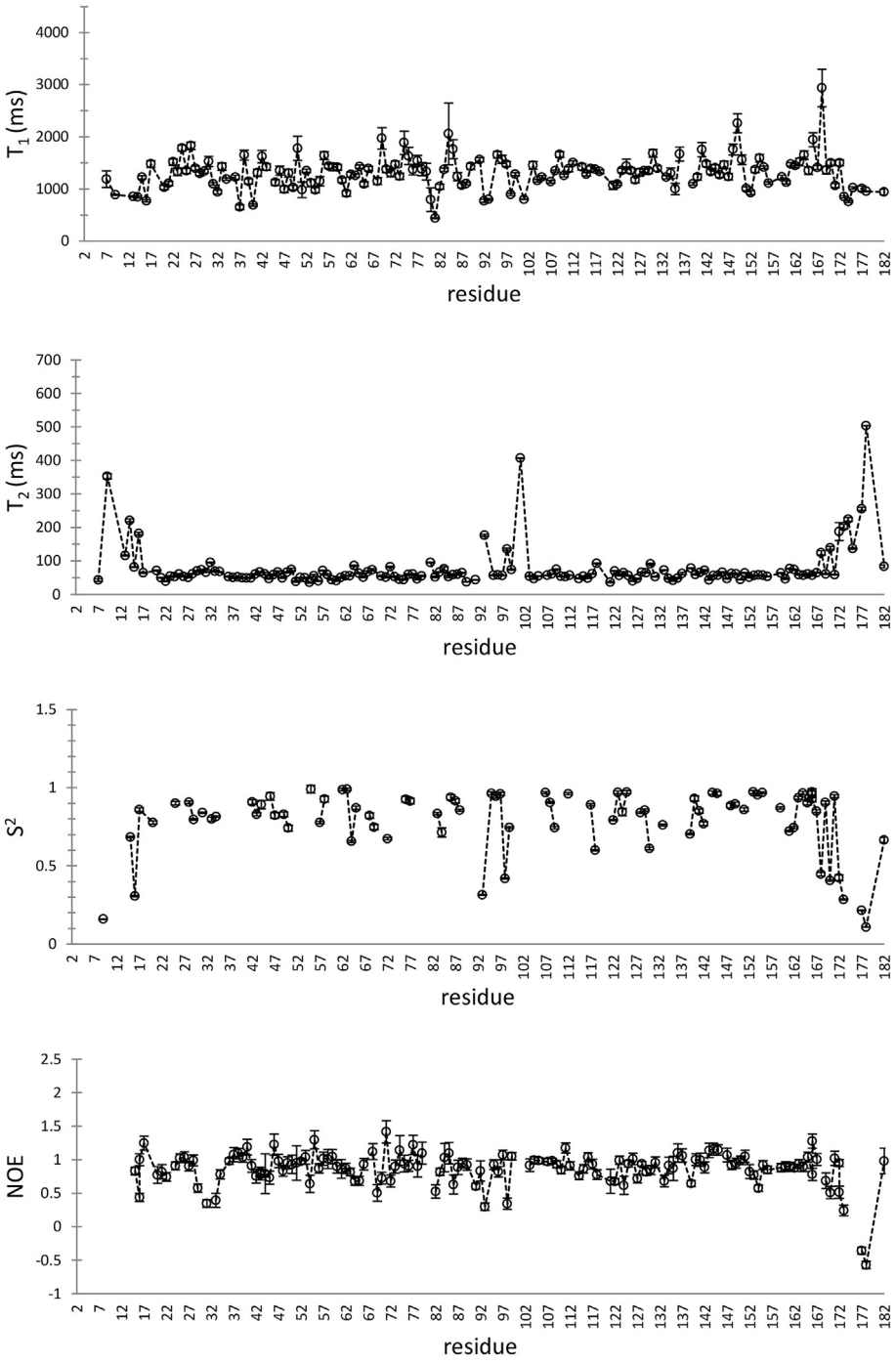

Fig. 8. Longitudinal (T_1) and transverse (T_2) relaxation times and steady state heteronuclear NOEs for ^{15}N,^{13}C, ^{2}H-labelled NS3pro with unlabelled NS2B and Bz-Nle-Lys-Arg-Arg-$B(OH)_2$. General order parameter squared (S^2) is fitted to the data by the Modelfree approach. Residue number is on the X-axis.

several conformations in the absence of inhibitor. Other NMR studies in the literature state that without inhibitor or substrate NS2B predominantly occupies the closed state [10,12,16,36]. Since the chemical shift changes upon addition of a strong inhibitor as shown in Fig. 6 are not dramatic, our data supports this theory.

3.6. Dynamics of NS2B and NS3pro in the presence of a peptidic inhibitor

To investigate backbone dynamics for unlinked NS2B-NS3pro in complex with Bz-Nle-Lys-Arg-Arg-$B(OH)_2$, longitudinal (T_1) and transverse (T_2) relaxation times and steady state heteronuclear NOEs were measured. The C-terminal residues of NS2B in complex with NS3pro and inhibitor are highly dynamic as shown by the low S^2 in Fig. 7. The negative charge character of this region, residues 89–94, is conserved across DENV NS2B, though not in WNV NS2B. It would be of interest to investigate if this dynamic region is of importance for e.g. substrate recognition. The flexibility of the C-terminus may also be a result of the truncation of NS2B. In native NS2B this loop is followed by a transmembrane region [37]. Based on the T_1 and T_2 values of NS2B the correlation time for molecular reorientation was 13 ns, which is in the expected range for a protein

with a molecular weight around 20 kDa. This suggests that NS2B is firmly associated with NS3pro when Bz-Nle-Lys-Arg-Arg-B$(OH)_2$ is bound. In the fast picosecond dynamic range (τE) there is no large differences between any of the measured amino acids except of A57 which also has a substantial error. ^{15}N CPMG-based relaxation dispersion experiments were applied to the NS2B-NS3pro – Bz-Nle-Lys-Arg-Arg-B$(OH)_2$ complex to study the microsecond to second timescale exchange processes (data not shown). No field strength dependence could be observed for any of the amino acids of the NS2B, demonstrating that binding of Bz-Nle-Lys-Arg-Arg-B$(OH)_2$ into the active site of NS3pro leads to the suppression of the slow dynamic mobility of the NS2B cofactor.

Backbone dynamics data for NS3pro are shown in Fig. 8. The N-terminal residues and the C-terminal residues of NS3pro are unstructured as shown by the low S^2. Based on the T_1 and T_2 values of NS3pro the correlation time for molecular reorientation was 12,8 ns, which corresponds well to the value calculated for NS2B, confirming that the two subunits of the NS2B-NS3pro complex move as one protein in solution. From the current data it is unclear which of the flexible termini is important for stability of NS3pro. As mentioned, we observed that truncNS3pro is less stable than full-length NS3pro. Similar to Kim et al. [10], we observed very similar spectra for NS3pro and truncNS3pro (data not shown). They selected a 14–185 construct over a 14–175 construct (very similar to truncNS3pro, 16–172), which would suggest that the flexible C-terminus is more important for stability than the N-terminus.

4. Conclusions

In this study, a new method is presented for production of functional, enzymatically active unlinked DENV NS2B-NS3pro complex. Several recent papers report co-expression of unlinked NS2B-NS3pro complexes [10,15], but we find that we can obtain high amounts of active complex by expressing them separately and co-refolding them using a very robust and easy protocol. Moreover, this method allows for differential domain labelling, thus facilitating the analysis of the different domains by e.g. NMR spectroscopy. Determining which conformations the NS2B cofactor can adopt in an uninhibited NS2B-NS3pro complex will be an interesting topic for future studies.

Author contributions

E.W. cloned, expressed and purified the protein, P.A. did the backbone resonance assignment, S. U. did the dynamics experiments and secondary chemical shift calculations, I. H. did the enzymology, and T. A. performed most NMR experiments.

Declaration of interests

This research did not receive any specific grant from funding agencies in the public, commercial, or not-for-profit sectors.

Acknowledgements

We thank J&J for valuable scientific discussions, and the rest of the dengue protease project team at Medivir.

Appendix A. Supplementary data

Supplementary data related to this article can be found at http://dx.doi.org/10.1016/j.pep.2017.07.002.

References

[1] N.M. Ferguson, et al., Benefits and risks of the Sanofi-Pasteur dengue vaccine: modeling optimal deployment, Science 353 (6303) (2016) 1033–1036.
[2] T.J. Chambers, C.S. Hahn, R. Galler, C.M. Rice, Flavivirus genome organization, expression and replication, Annu. Rev. Microbiol. 44 (1990) 649–688.
[3] B. Falgout, et al., Both nonstructural proteins NS2B and NS3 are required for the proteolytic processing of dengue virus nonstructural proteins, J. Virol. 65 (5) (1991) 2467–2475.
[4] P. Erbel, et al., Structural basis for the activation of flaviviral NS3 proteases from dengue and West Nile virus, Nat. Struct. Mol. Biol. 13 (4) (2006) 372–373.
[5] C.G. Noble, et al., Ligand-bound structures of the dengue virus protease reveal the active conformation, J. Virol. 86 (1) (2012) 438–446.
[6] P. Niyomrattanakit, et al., Identification of residues in the dengue virus type 2 NS2B cofactor that are critical for NS3 protease activation, J. Virol. 78 (24) (2004) 13708–13716.
[7] W.Y. Phong, et al., Dengue protease activity: the structural integrity and interaction of NS2B with NS3 protease and its potential as a drug target, Biosci. Rep. 31 (5) (2011) 399–409.
[8] R. Yusof, S. Clum, M. Wetzel, H.M. Krishna Murthy, R. Padmanabhan, Purified NS2B/NS3 serine protease of dengue virus type 2 exhibits cofactor NS2B dependence for cleavage substrates with dibasic amino acids in vitro, J. Biol. Chem. 275 (14) (2000) 9963–9969.
[9] I. Radichev, et al., Structure-based mutagenesis identifies important novel determinants of the NS2B cofactor of the West Nile virus two-component NS2B-NS3 proteinase, J. Gen. Virol. 89 (Pt 3) (2008) 636–641.
[10] Y.M. Kim, et al., NMR analysis of a novel enzymatically active unlinked dengue NS2B-NS3 protease complex, J. Biol. Chem. 288 (18) (2013) 12891–12900.
[11] L. de la Cruz, et al., Binding mode of the activity-modulating C-terminal segment of NS2B to NS3 in the dengue virus NS2B-NS3 protease, FEBS J. 281 (6) (2014) 1517–1533.
[12] X.C. Su, et al., NMR analysis of the dynamic exchange of the NS2B cofactor between open and closed conformations of the West Nile virus NS2B-NS3 protease, PLoS Negl. Trop. Dis. 3 (12) (2009) e561.
[13] D. Leung, et al., Activity of recombinant dengue 2 virus NS3 protease in the presence of a truncated NS2B co-factor, small peptide substrates, and inhibitors, J. Biol. Chem. 276 (49) (2001) 45762–45771.
[14] S. Clum, K.E. Ebner, R. Padmamabhan, Cotranslational membrane insertion of the serine proteinase precursor NS2B-NS3(pro) of dengue virus type 2 is required for efficient in vitro processing and it mediated through the hydrophobic regions of NS2B, J. Biol. Chem. 272 (49) (1997) 30715–30723.
[15] A.E. Shannon, et al., Simultaneous uncoupled expression and purification of the Dengue virus NS3 protease and NS2B co-factor domain, Protein Expr. Purif. 119 (2016) 124–129.
[16] G. Gupta, L. Lim, J. Song, NMR and MD studies reveal that the isolated dengue NS3 protease is an intrinsically disordered chymotrypsin fold which absolutely requests NS2B for correct folding and functional dynamics, PLoS One 10 (8) (2015) e0134823.
[17] Y.P.D. Cheng, An efficient system for small protein expression and refolding, Biochem. Biophys. Res. Commun. 317 (2) (2004) 401–405.
[18] J. Sambrook, E.F. Fritsch, T. Maniatis, Molecular Cloning: a Laboratory Manual (3 Volume Set) 2nd Edition, second ed., 1989.
[19] S. van den Berg, et al., Improved solubility of TEV protease by directed evolution, J. Biotechnol. 121 (3) (2006) 291–298.
[20] Z. Yin, et al., Peptide inhibitors of Dengue virus NS3 protease. Part 1: Warhead, Bioorg Med. Chem. Lett. 16 (1) (2006) 36–39.
[21] S. Unnerstale, et al., Backbone assignment of the MALT1 paracaspase by solution NMR, PLoS One 11 (1) (2016) e0146496.
[22] K. Pervushin, et al., Attenuated T2 relaxation by mutual cancellation of dipole-dipole coupling and chemical shift anisotropy indicates an avenue to NMR structures of very large biological macromolecules in solution, Proc. Natl. Acad. Sci. U. S. A. 94 (23) (1997) 12366–12371.
[23] A. Eletsky, A. Kienhofer, K. Pervushin, TROSY NMR with partially deuterated proteins, J. Biomol. NMR 20 (2) (2001) 177–180.
[24] T. Schulte-Herbruggen, O.W. Sorensen, Clean TROSY: compensation for relaxation-induced artifacts, J. Magn. Reson 144 (1) (2000) 123–128.
[25] M. Salzmann, et al., TROSY in triple-resonance experiments: new perspectives for sequential NMR assignment of large proteins, Proc. Natl. Acad. Sci. U. S. A. 95 (23) (1998) 13585–13590.
[26] M. Salzmann, et al., Improved sensitivity and coherence selection for [15N,1H]-TROSY elements in triple resonance experiments, J. Biomol. NMR 15 (2) (1999) 181–184.
[27] W.F. Vranken, et al., The CCPN data model for NMR spectroscopy: development of a software pipeline, Proteins 59 (4) (2005) 687–696.
[28] S. Schwarzinger, et al., Random coil chemical shifts in acidic 8 M urea: implementation of random coil shift data in NMRView, J. Biomol. NMR 18 (1) (2000) 43–48.
[29] G. Zhu, et al., Protein dynamics measurements by TROSY-based NMR experiments, J. Magn. Reson 143 (2) (2000) 423–426.
[30] M. Tollinger, et al., Slow dynamics in folded and unfolded states of an SH3 domain, J. Am. Chem. Soc. 123 (46) (2001) 11341–11352.
[31] D.S. Wishart, B.D. Sykes, F.M. Richards, The chemical shift index: a fast and simple method for the assignment of protein secondary structure through

NMR spectroscopy, Biochemistry 31 (6) (1992) 1647–1651.
[32] A. D'Arcy, et al., Purification and crystallization of dengue and West Nile virus NS2B-NS3 complexes, Acta Crystallogr. Sect. F. Struct. Biol. Cryst. Commun. 62 (Pt 2) (2006) 157–162.
[33] K. Pervushin, et al., [15N,1H]/[13C,1H]-TROSY for simultaneous detection of backbone 15N-1H, aromatic 13C-1H and side-chain 15N-1H2 correlations in large proteins, J. Biomol. NMR 17 (3) (2000) 195–202.
[34] A. Liu, et al., TROSY of side-chain amides in large proteins, J. Magn. Reson 186 (2) (2007) 319–326.
[35] C. Nitsche, et al., Peptide-boronic acid inhibitors of flaviviral proteases: medicinal chemistry and structural biology, J. Med. Chem. 60 (1) (2017) 511–516.
[36] L. de la Cruz, et al., Binding of low molecular weight inhibitors promotes large conformational changes in the dengue virus NS2B-NS3 protease: fold analysis by pseudocontact shifts, J. Am. Chem. Soc. 133 (47) (2011) 19205–19215.
[37] Q. Huang, et al., Lyso-myristoyl phosphatidylcholine micelles sustain the activity of Dengue non-structural (NS) protein 3 protease domain fused with the full-length NS2B, Protein Expr. Purif. 92 (2) (2013) 156–162.
[38] M.S. Cheung, et al., DANGLE: a Bayesian inferential method for predicting protein backbone dihedral angles and secondary structure, J. Magn. Reson 202 (2) (2010) 223–233.

Web references

[1a] http://www.who.int/denguecontrol/resources/9789241504034/en/, Source: World Health Organization, Author: R. Velayudhan, Publication date: August 2012, ISBN 9789241504034.
[1b] http://www.sanofipasteur.com/en/articles/first_dengue_vaccine_approved_in_more_than_10_countries.aspx, Source: Sanofi Pasteur, Publication date: October 4, 2016, Accessed: 14 June 2017.